Scientific paper

Electrochemical Impedance Spectroscopy as a Tool in the Plate Making Process Optimization

Tomislav Cigula,[1,*] Regina Fuchs-Godec,[2] Miroslav Gojo[1] and Mojca Slemnik[2]

[1] *University of Zagreb, Faculty of Graphic Arts, Getaldiceva 2, Zagreb, Croatia*

[2] *University of Maribor, Faculty of Chemistry and Chemical Engineering*

* *Corresponding author: E-mail: tcigula@grf.hr*

Received: 20-01-2012

Dedicated to Prof. Dr. Gorazd Vesnaver on the occasion of his 70th birthday

Abstract

The structure of the porous aluminium-oxide layer, which builds non-image areas, has the most significant influence on the quality of final graphical product. This paper presents the results of the application of EIS in the characterisation and detection of changes on the aluminium-oxide layer caused by chemical processing in highly alkaline solution. The Al_2O_3 layer was characterised using SEM, fractal dimension and surface free energy calculation and EIS analysis. The results of the investigation showed that chemical processing has a significant influence on the structure of aluminium-oxide which could lead to a decrease in the quality of the printing plate. EIS enables the detection of changes on the aluminium-oxide layer. The two equivalent circuits are proposed. Based on modelling with the obtained EIS spectra, precise evaluation of developing time in which complete removal of the photoactive layer is achieved. This makes EIS a powerful tool in optimizing chemical processing of lithographic printing plates.

Keywords: Printing plate, chemical processing, SEM, surface free energy, EIS

1. Introduction

Offset printing is the main representative of lithography, determined by indirect transfer of printing ink from the printing plate to the printing substrate.[1] Selective adsorption of printing ink on the printing plate is achieved by the opposite surface properties of the image and non-image areas. Image areas are made of organic coating, which makes them oleophilic and hydrophobic while non-image areas are built of aluminium-oxide, which makes them hydrophilic and enables good adsorption of water based fountain solution.[2]

Lithographic printing plates are usually made of aluminium foils. To improve the adhesion of fountain solution and photoactive coating in the printing process, the aluminium foil is mechanically, chemically and electrochemically processed (grained) to make a defined rough surface.[3–5] Anodic oxidation is performed after graining to build a thin aluminium-oxide layer which consists of a compact layer (barrier layer) and an outer porous layer.[6] The printing performance and the durability of the printing plate are influenced considerably by the formed surface structure of the aluminium foil.[7–8] The aluminium foil is after processing covered with a thin (2–3 μm) photoactive layer.[9]

The plate making process consists of two processes, exposure where the plate is irradiated by a defined light source and developing process. The exposure must induce a chemical reaction in the photoactive layer, which will make it soluble (positive working) or insoluble (negative working) in the defined solution (developer). The developing process must remove parts of the photoactive layer completely, thus opening the processed aluminium foil surface which builds non-image areas.[10]

Majority of photoactive layers used today use high alkaline solution (pH ≈13) as a developer. Having in mind the amphoteric character of aluminium-oxide it could be assumed that the developing process could induce changes of the aluminium-oxide topography that may impair the quality of printing plates. The developing process

must therefore be conducted under strict conditions which enable removal of the photoactive layer, but minimize the influence on aluminium-oxide.

Electrical Impedance Spectroscopy (EIS) had already been used for the characterization of different porous surfaces.[11–16] This paper presents the results of EIS application in determining the changes in the non-image surface of the printing plate, caused by processing in defined developer. Influence of developing time on the surface characteristics and the possibility to optimize this process is investigated by observing differences in impedance spectra and proposed equivalent circuits.

2. Experimental

2. 1. Sample Preparation

The printing plates used in this research are conventional printing plates coated with positive diazo photoactive layer, which are used in the conventional and the Computer to Conventional Plate making system. Both of these plate making processes include developing of the plate in an alkaline solution. The aluminium foil was processed according to prior reported process,[4–7] including a two step anodic oxidation. In the first step the foil is cathode, while in the second step it is anode.

Samples of printing plates were exposed with the PlurimetalEXPO74 unit equipped with a 3.5 kW metal-halide lamp for 60 pulses (the unit measures the pulse energy and compensates the reduction of lamp intensity over time). After exposure, samples were developed in the solution of 0.2 mol L^{-1} NaOH. Developer was prepared by dissolving NaOH p.a. crystals in distilled water (INA, ISO 9001, ISO 14001, OHSAS 18001). Seven samples of printing plates were prepared by extending the developing time from 5 to 29 seconds with the difference of 4 seconds. Samples were noted as S_1– S_7, where the higher index number signifies longer developing time. In order to eliminate the influence of temperature and saturation of developer, all samples were developed at temperature of 25 ± 0.1 °C in freshly prepared developer. After the developing process all samples were washed in distilled water.

2. 2. Measuring Methods and Equipment

EIS measurements of printing plates were performed by the Princeton Applied Research VersaSTAT3 potentiostat in a standard three electrode electrochemical cell. The electrochemical cell consists of saturated calomel electrode (SCE), graphite counter electrode and working electrode (plate samples). The measurements were conducted in accordance with the procedure detailed in the previous research.[13–15,17–18] The samples of 16 mm diameter were fixed in sample holder and immersed in unstirred, aerated solution of 0.2 mol L^{-1} concentrated K_2SO_4. The sample area which was in contact with the solution was 1 cm^2. EIS spectra were measured within the 100 kHz –10 mHz frequency range at open circuit potential. The amplitude of excitation voltage was 10 mV. The results of the measurement were further analysed by the EChem Software's ZSimpWin 3.21 software, which enables the modelling of EIS spectra with desired equivalent circuit.[19]

SEM micrographs of investigated samples were obtained with JEOL JSM-6460 scanning electron microscope. To assure uniform electrical properties of the samples and to avoid charging/discharging of the aluminium-oxide surface, the plate samples were gold coated by the Baltec SCD 005 sputtering unit.

Estimation of the fractal dimension of the SEM micrographs was made using the Gwiddion image analysis software. This software enables image correction and the calculation of fractal dimension using various methods.

Surface free energy of the investigated samples was determined indirectly by measuring contact angle of standard liquids with known surface tension values (Table 1).

Table 1: Surface tension of the standard liquids

Liquid	Surface tension (mN/m)	Surface tension's dispersive part (mN/m)	Surface tension's polar part (mN/m)	The author of surface tension value
Redistilled water, γ = 2.0 μS cm^{-1}	72.8	21.8	51	Ström et al.[22]
Glycerol	64	34	30	Van Osset al.[23]
Diiodo-methane	58.8	50.8	0	Strömet al.[22]

Calculation of the surface free energy was done using Owens, Wendt Rabel and Kaelbe method (OWRK) which enables determination of polar and dispersive part of surface free energy.[20] This method is recommended when analysing surfaces similar to the printing plate.[21] Measurement of the contact angle was performed by Dataphysics's OCA30 goniometer. The contact angle was determined using the Sessile drop method. Analysis of the liquid drop was performed by Dataphysics' SCA20 software using ellipse/Laplace-Young fitting depending on the drop shape.

3. Results and Discussion

The micrographs presented in Figure 1 show the structure of aluminium-oxide surface. In Figure 1a large dark areas can be seen, which were caused by the incomplete removal of the photoactive layer. The amount of darker areas is decreasing with the increase of the developing

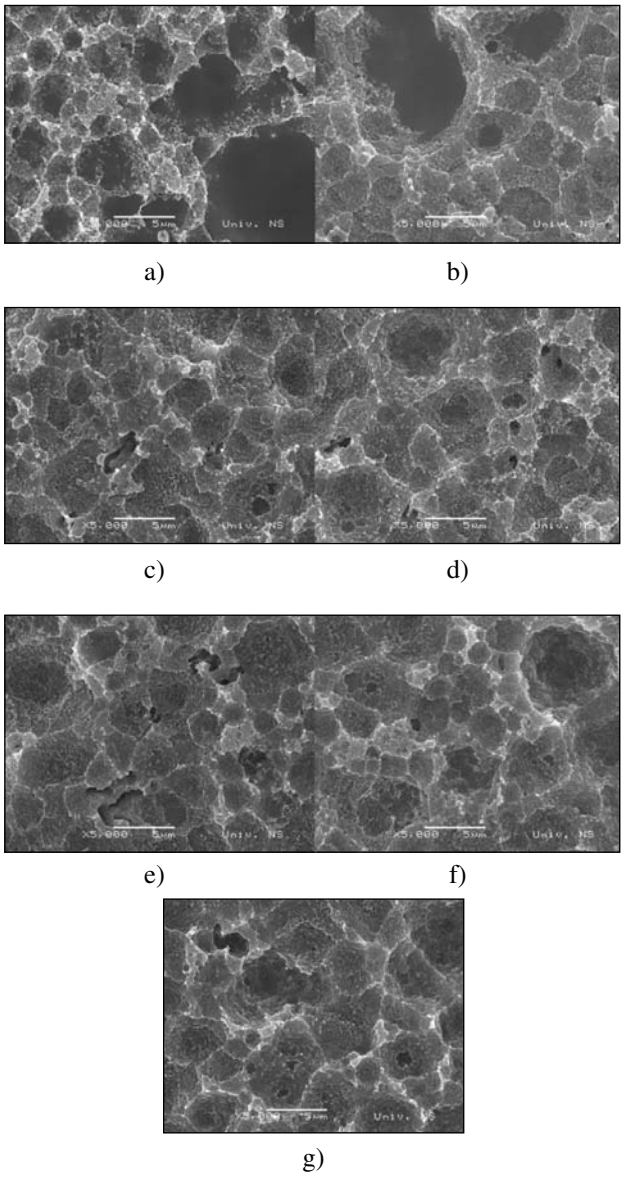

a) b) c) d) e) f) g)

Figure 1: SEM micrographs at magnification 5000×
a) S_1, b) S_2, c) S_3, d) S_4, e) S_5, f) S_6 g) S_7

time (Figures 1b and 1c) to complete disappearing. The structure of the aluminium-oxide seen in Figures 1d-1g is characterised with relatively large and shallow pores with present self similarity (fractal structure). One could see in Figures 1d–1g structures without self similarity. These structures probably originate from dissolved impurities which are likely to have been built in the aluminium-oxide layer during anodic oxidation.

Results of the surface free energy calculation are shown in Figure 2. Dots in the diagram represent measured values and lines present polynomial fit.

One could see that surface free energy is increasing to the developing time of 17 seconds (S_4). A further increase in the developing time results in lower values of the surface free energy (Figure 2). Furthermore, the change of

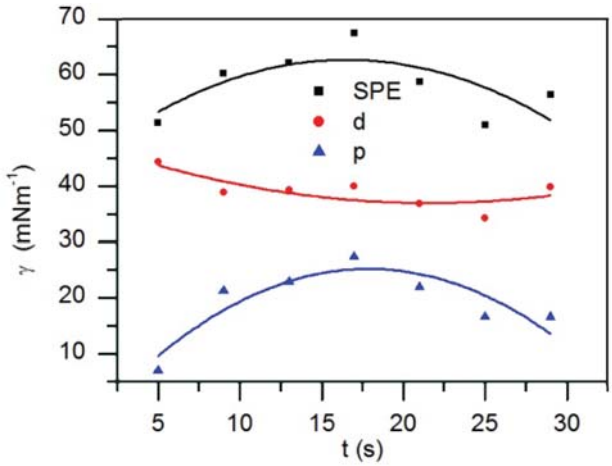

Figure 2: Surface free energy values (SPE), its dispersive (d) and polar (p) part of investigated samples

value of surface free energy is influenced more by the change of its polar part than its dispersive part.

The aluminium-oxide surface is polar, so the increase of the polar part of surface free energy is the consequence of the removalof organic compound (photoactive layer) off the aluminium-oxide surface. After reaching the highest value, surface free energy decreases its value due to the smoothening of the surface caused by the dissolution of aluminium-oxide.

Fractal dimension was determined on SEM micrographs at magnification 5000× as previous research showed its independence on magnification.[24]

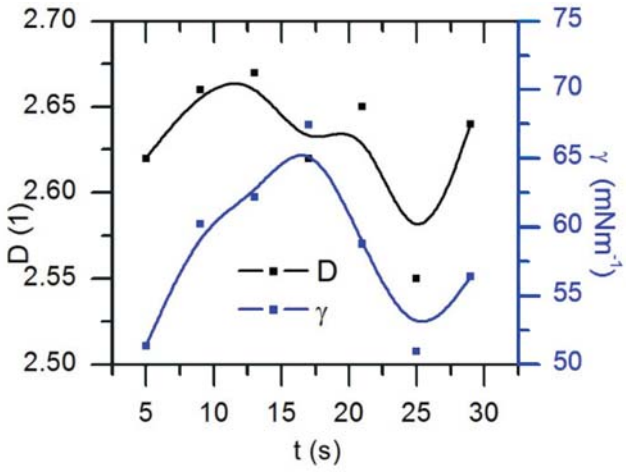

Figure 3: Fractal dimension (D) and surface free energy (γ) of investigated samples

Previous research proved that fractal dimension can give an insight into the surface texture as there is a high correlation factor between the fractal dimension and roughness parameters.[25] The correlation between the results of the fractal dimension and the surface free energy

can indicate the influence of surface texture on the surface free energy value.

The value of the fractal dimension increases by extending the developing time of the printing plate until reaching the highest value at the developing time of 13 seconds. This behaviour suggests that the aluminium-oxide surface is partly covered with photoactive coating at lower developing times. After dissolving the photoactive layer, the developing solution starts dissolving the aluminium-oxide and thereby flattens the surface of the printing plate, i.e. the fractal dimension decreases.

Correlation between the surface free energy values and the fractal dimension is very high in low (5–13 s) and the high (21–29 s) developing time with correlation coefficients (calculated using Pearson method) of 0.999 and 0.977, respectively. A small decrease in the correlation between the high and low developing time, as well as the difference at S_4 (17 s) could be the consequence of measuring method resolution. It should be noted that the fractal dimension has resolution to the nano-scale while droplets at contact angle measurements are micro-scale. The difference in the resolution enables the fractal dimension to detect even the smallest artefacts in the aluminium-oxide layer, which are seen in SEM micrographs (Figures 1d–1g).

Results of EIS are shown in Figure 4. One could see that value of the impedance is decreasing with the increase of the developing time.

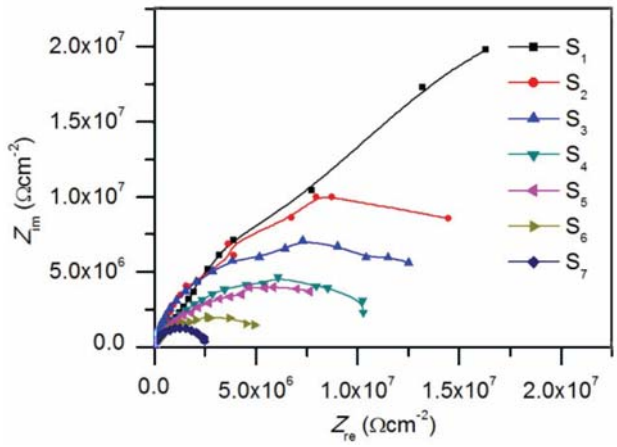

Figure 4: Nyquist diagrams of impedance spectrum measured on investigated printing plate samples

The obtained results of the EIS measurements were modelled using two types of equivalent circuits shown in Figure 5.

These proposed equivalent circuits are based on previous researches induced by aluminium-oxide properties.[16,18,26–27] The CPE element was introduced instead of the simple capacity to allow changes in the porous layer due to the interaction with the processing solution. The impedance of a constant phase element (CPE) is defined as:

$$Z_{CPE} = [Q\,(j\omega)^n]^{-1} \quad (1)$$

where Q is the frequency – dependent element and is a combination of properties related both to the surface and the electroactive species. The exponent n is related to a slope of the log Z vs. log f in Bode plot, i.e., to the phase angle θ by the relationship $n = 2\theta\pi^{-1}$; $j = (-1)^{0.5}$. ω is the angular frequency. The parameter Q ($s^n\Omega^{-1}$ cm^{-2}) can be converted into capacitance C($s\Omega^{-1}$ cm^{-2}) when $n < 1$, which is especially important when experimental data are used to determine quantitatively system parameters such as thickness or dielectric constant.

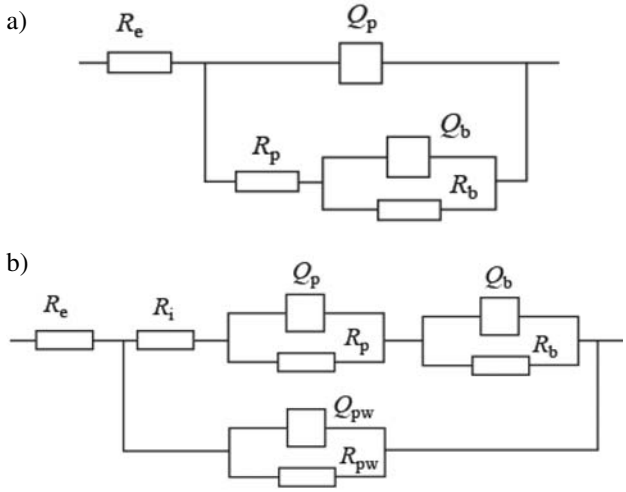

Figure 5: Equivalent circuit a) *Ladder* type circuit, b) closed pore model where: R_e – electrolyte resistance, R_p – pore resistance, R_b – barrier layer resistance, R_{pw} – pore wall resistance, R_i – resistance of the intermediate layer, Q_p – pore CPE element, Q_b – barrier layer CPE element, Q_{pw} – pore wall CPE element

The modelling showed good fitting of the closed pore model equivalent circuit on the samples S_1– S_3 while *Ladder* type equivalent circuit was used on other samples. The use of the closed pore model is appropriate when the developing time is not long enough to dissolve the photoactive layer in the pores of the aluminium-oxide layer. The Ladder type equivalent circuit could be used for fitting when the photoactive layer is removed from the pores.

Figure 6 shows diagrams of modelling results of impedance data measured on S_1–S_3 with the closed pore model (Figure 6a) and S_4–S_7 with the Ladder equivalent circuit (Figure 6b). The points in diagrams represent measured values, and lines represent calculated values.

The values of EC parameters calculated by the modelling of EIS results with the proposed equivalent circuits on the investigated samples are presented in tables 2 and 3.

It can be noticed that the values of the R_i and R_p parameters are decreasing with the extension of the developing time. The parameters connected with the barrier la-

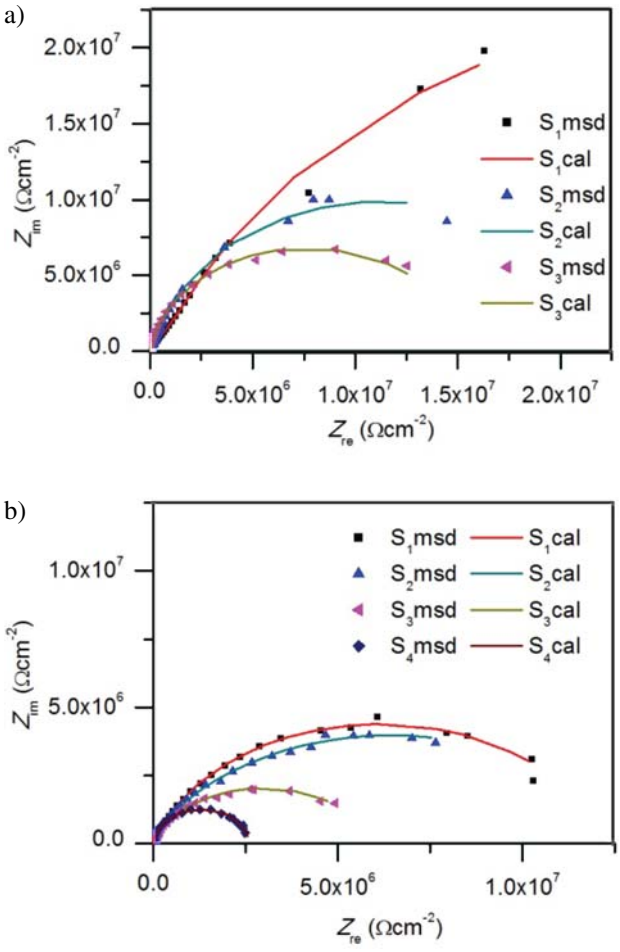

Figure 6: Nyquist plots of modelling with a) closed pore model, b) Ladder type circuit

Table 2: EC parameters calculated using the closed pore model

	Sample		
	S_1	S_2	S_3
R_e (Ω cm^{-2})	17.7	10.7	10.0
Q_w (Ss^n cm^{-2})	6.7 10^{-8}	2.2 10^{-7}	2.6 10^{-7}
n_w	0.80	0.88	0.95
R_w (Ω cm^{-2})	8 10^{10}	1.1 10^9	3.6 10^9
R_i (Ω cm^{-2})	1.1 10^5	9.7 10^4	5.7 10^4
Q_p (Ss^n cm^{-2})	2.6 10^{-7}	2.1 10^{-7}	2.6 10^{-7}
n_p	0.80	0.66	0.80
R_p (Ω cm^{-2})	6.2 10^7	1.5 10^6	9.6 10^4
Q_b (Ss^n cm^{-2})	2.6 10^{-7}	2.3 10^{-7}	1.0 10^{-7}
n_b	0.80	0.99	0.85
R_b (Ω cm^{-2})	1.2 10^6	2.1 10^7	1.5 10^7

yer (Q_b and R_b) are nearly constant on the investigated samples. These results confirm the assumption that the developing solution starts to dissolve the porous layer of aluminium-oxide when the photoactive layer is removed from its surface.

Table 3: EC parameters calculated using the Ladder type circuit

	Sample			
	S_4	S_5	S_6	S_7
R_e (Ω cm^{-2})	15.9	11.8	11.0	10.5
Q_p (Ss^n cm^{-2})	1.1 10^{-7}	1.6 10^{-7}	1.2 10^{-7}	4.5 10^{-7}
n_p	0.96	0.80	1.0	0.97
R_p (Ω cm^{-2})	3.3 10^4	1.6 10^4	4.1 10^3	2.7 10^2
Q_b (Ss^n cm^{-2})	1.6 10^{-7}	2.9 10^{-7}	3.5 10^{-7}	3.6 10^{-7}
n_b	0.70	0.80	0.69	0.97
R_b (Ω cm^{-2})	1.2 10^7	1.4 10^7	6.2 10^7	2.6 10^7

As the models present a parallel connection of the resistance and the CPE element, it is possible to calculate the capacitance of double layer:[28]

$$C_{dl} = \sqrt[n]{\frac{Q}{R_{ct}^{n-1}}} \quad (2)$$

where C_{dl} is the capacitance of double layer, Q and R_{ct} and n are the values of the parameters in the R–Q parallel connection.

Figure 7 shows the dependence of pore resistance (R_p) and pore capacitance C_p on the developing time. It is evident that the pore resistance continuously decreases with the extension of the developing time. The decrease of resistance value is substantial in the lower developing times (5–13 s), but it continues to drop to the lowest value at the developing time of 29 s. On the other hand, C_p is slightly decreasing till the developing time of 25 s.

The decrease of the pore resistance is probably caused by opening the pores after the removal of the photoactive layer, which has a compact structure. When the photoactive layer is removed, there are two possible mechanisms, the absorption of water to create hydrated aluminium-oxide[29–30] and the filling of the pores with electroly-

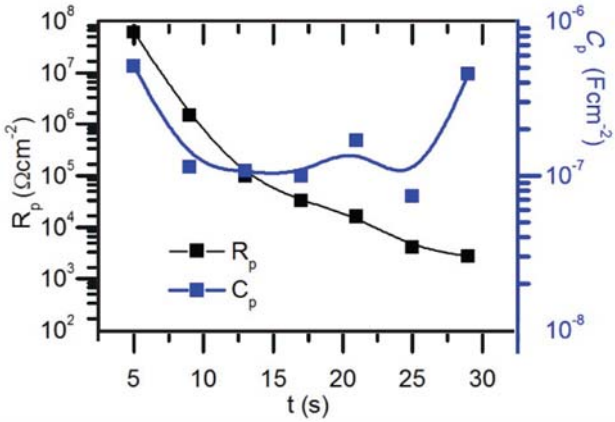

Figure 7: Pore resistance (R_p) and pore capacitance (C_p) depending on developing time

te when pores are open. This effect is dominant in the lower developing time. The pore resistance value decreases rapidly in the lower developing time (5–17s), after which decrease of the resistance value is slight. This behaviour could be attributed to the change of the dominant mechanism influencing pore resistance. The first high pore resistance is probably the result of the pores partially filled with the photoactive layer. After the complete removal of the photoactive layer, the developer is dissolving aluminium-oxide layer, causing the deterioration of its surface. The decrease in capacitance is probably caused by the absorption of water into the aluminium-oxide structure which is also seen in the decrease of the resistance value. The increase of the C_p value on the sample S_7 could be the consequence of the dissolution of aluminium-oxide, which probably causes the increase of micro roughness, also seen in the increase of the fractal dimension.

4. Conclusions

This research was made to evaluate the use of EIS in detecting surface changes of the non-image areas of the printing plate, induced by the developing process. Although the developing process should not have any influence on the quality of the printing plate, the amphoteric character of aluminium-oxide indicates that it could be dissolved by a high alkaline developer.

The results have proven that the surface structure of aluminium-oxide changes with the alteration of the developing time. If the developing time is too short, the remains of the photoactive layer causes lower surface free energy and its polar part, probably resulting in a worse adsorption of fountain solution in the printing process. The longer developing time causes dissolution of the aluminium-oxide and smoothening of the surface, which also results in a lower adsorption of fountain solution.

The obtained impedance spectra were successfully modelled with the proposed equivalent circuits corresponding to the anodized layer with closed pore, including an intermediate layer, and to the open pore structure. As the developer used for processing of the printing plate was fresh, the intermediate layer probably presents the remains of the photoactive layer. The change of the appropriate equivalent circuit model indicates the developing time in which photoactive layer is completely removed from the non-image areas. In addition, the behaviour of pore resistance and capacitance corroborate proposed mechanisms which occur in the developing process after the removal of the photoactive layer, the degradation of surface roughness induced by dissolution of the aluminium-oxide and water absorption in the pores resulting in a sealing process.

In conclusion, it can be stated that EIS has proved to be a powerful tool in detecting structural change of the porous aluminium-oxide layer caused by the developing process enabling precise determination of the optimal developing time which would result with high quality printing plate, consequently final printed product.

5. Acknowledgements

This work was supported by the Croatian Ministry of Science, Education and Sports, Grant No.: 128-1201785-2228 "The development of methods for printing plates surface measurements" and by the bilateral Croatian-Slovenian project "Electrochemical study and corrosion resistance of aluminium and aluminium oxide and its application on the offset printing forms". The authors would like to thank Mr. Milos Bokorov (University of Novi Sad, Centre for Microscopy) for the SEM micrographs of the samples.

6. References

1. S. Bolanca. Glavnetehniketiska, ActaGraphica, **1997**.
2. D. G. Wilson. Lithography primer, GATFPress, **2005**.
3. O. Gobbetti, Electrochemical Graining of Aluminum or Aluminum Alloy Surfaces, Patent No.: US 5,064,511, November 12, **1991.**
4. C. S. Lin, C. C. Chang, H. M. Fu, *Mater. Chem. Phys.* **2001**, *68*, 217–224.
5. P. K. F. Limbach, M. P. Amor, J. Ball, Aluminium Sheet with Rough Surface, Patent No.: US 6,524,768 B1, date of patent February 25, **2003.**
6. A. Nishino, Y. Masuda, H. Sawada, A. Uesugi, Process for Producing Aluminum Support for Lithographic Printing Plate, Patent No.: US 6,682,645 B2, January 27, **2004**.
7. Th. Dimogerontakis, S. Van Gils, H. Ottevaere, H. Thienpont, H. Terryn, *Surf. Coat. Technol.* **2006,** *201,* 918–926.
8. B. Rivetta, E. V. Korolevaa, F. J. Garcia-Garcia, J. Armstrong, G. E. Thompson, P. Skeldon, *Wear* **2011**, *270*, 204–217.
9. T. Urano, K. Kohori, H. Okamoto, Photosensitive Lithographic Printing Plate and Method for making a Printing Plate, Patent No.: US 6,689,537 B2, date of patent February 10, **2004**.
10. H. Kipphan. Handbook of Print Media, Springer, **2001**.
11. J. J. Suay, E. Giménez, T. Rodríguez, K. Habbib, J. J. Saura,*Corros. Sci.* **2003**, *45*, 611–624.
12. J. A. Gonzalez, V. Lopez, A. Bautista, E. Otero, X.R. Növoa, *J. Appl. Electrochem.* **1999**, *29*, 229–238.
13. B. van der Linden, H. Terryn, J. Vereecken, *J. Appl. Electrochem.* **1990**, *20*, 798–803.
14. J. De Laet, J. Scheers, H. Terryn, J. Vereecken, *Electrochim. Acta***1993**, *38*, 2103–2109.
15. J. A. Gonzalez, V. Lopez, E. Otero, A. Bautista, *J. Electrochem. Soc.* **2000**, *147*, 984–990.
16. S. MahovicPoljacek, D. Risovic, T. Cigula, M. Gojo, *J. Solid State Electrochem.* **2012***, 16,* 1077–1089.

17. W. Rauh, S. Dietzel, A. Sandow. Electrochemische Untersuchungen der Oberfläche vonOffset druck plattenzur Aufklärung der Ursachen von Farbannahmeerscheinungenanbildfreein Stellen, FOGRA Forschungsgesellschaft Drucke.V., **2006.**
18. J. Hitzig, K. Jüttner, W. J. Lorenz, W. Paatsch, *Corros. Sci.* **1984**, *24*, 945–952.
19. B. Yeum. ZSimpWin Version 3.20, User manual, Princeton Applied Research, **2004.**
20. D. K. Owens, R.C. Wendt, *J. Appl. Polym. Sci.* **1969**, *13*, 1741–1747.
21. Data Physics Instruments GmbH. Operating manual OCA, **2006**.
22. G. Ström, M. Frederikson, P. Stenius, *J. Colloid Interf. Sci.***1987**,*119*, 352–361
23. C. J. Van Oss, R. F Giese, W. Wu, *J. Adhes.***1997**, *63*, 71–88
24. D. Risovic, S. Mahovic Poljacek, K. Furic, M. Gojo, *Appl. Surf. Sci.* **2008**, *255,* 3063–3070.
25. D. Risovic, S. Mahovic Poljacek, M. Gojo, *Appl. Surf. Sci.* **2009**, *255*, 4283–4288.
26. F. Debuyck, L. Lemaitre, M. Moors, A.P. Van Peteghem, E. Wettinck, L. Weyten, *Surf. Coat. Technol.* **1988**, *34*, 311–318.
27. F. J. Martin, G. T. Cheek, W. E. O'Grady, P. M. Natishan, *Corros. Sci.* **2005**, *47*, 3187–3201.
28. S. Martinez, M. Metikos-Hukovic, *J. Appl.Electrochem.* **2003**, *33*, 1137–1142.
29. R. Lizarbe, J. A. González, E. Otero, V. López, *Alum.* **1993**, *69*, 548–552.
30. J. A. González, V. López, E. Otero, A. Bautista, R. Lizarbe, C. Barba, J. L. Baldonedo, *Corros. Sci.* **1997**, *39*, 1109–1118.

Povzetek

Struktura porozne plasti aluminijevega oksida, ki predstavlja t.i. tiska prosto površino ima pomemben vpliv na kvaliteto tiska. Delo predstavlja uporabo impedančne spektroskopije (EIS) v namene detekcije strukturnih sprememb povzročenih pri kemijski obdelavi površine v močno alkalni raztopini. Strukturne spremembe plasti aluminijevega oksida, nastale v procesu delovanja razvojnega medija na površino smo razložili še z uporabo SEM, fraktalne analize in merjenjem površinske energije. Analize so pokazale, da ima proces kemijske obdelave tiskarske plošče bistven vpliv na končno kvaliteto le-te. S pomočjo EIS lahko uspešno predvidimo spremembe v plasti aluminijevega oksida. Uporabili smo dva različna tipa nadomestnega električnega vezja. Na osnovi le-teh smo lahko natančno predvideli optimalni čas razvijanja pri katerem je bil foto-aktivni film odstranjen v celoti. Vse to daje velik pomen uporabi EIS v namene optimizacije kemijskega procesa v postopku priprave litografskih tiskarskih plošč.